

SKATER: Synthesized Kinematics for Advanced Traversing Efficiency on a Humanoid Robot via Roller Skate Swizzles

Junchi Gu, Feiyang Yuan, Weize Shi, Tianchen Huang, Haopeng Zhang, Xiaohu Zhang, Yu Wang, Wei Gao and Shiwu Zhang

Abstract—Although recent years have seen significant progress of humanoid robots in walking and running, the frequent foot strikes with ground during these locomotion gaits inevitably generate high instantaneous impact forces, which leads to exacerbated joint wear and poor energy utilization. Roller skating, as a sport with substantial biomechanical value, can achieve fast and continuous sliding through rational utilization of body inertia, featuring minimal kinetic energy loss. Therefore, this study proposes a novel humanoid robot with each foot equipped with a row of four passive wheels for roller skating. A deep reinforcement learning control framework is also developed for the swizzle gait with the reward function design based on the intrinsic characteristics of roller skating. The learned policy is first analyzed in simulation and then deployed on the physical robot to demonstrate the smoothness and efficiency of the swizzle gait over traditional bipedal walking gait in terms of Impact Intensity and Cost of Transport during locomotion. A reduction of 75.86% and 63.34% of these two metrics indicate roller skating as a superior locomotion mode for enhanced energy efficiency and joint longevity.

I. INTRODUCTION

Recent advances in locomotion control of legged robots have yielded remarkable movement strategies, including walking [1], running [2], jumping [3] and dancing [4]. However, these motions often impose extreme demands on joint actuator torque and velocity, undertake significant joint impacts during execution and produce substantial noises. Specifically, in walking and running gaits, robots experience intermittent ground contacts with considerable instantaneous impact forces at each touchdown. This not only accelerates joint wear but also substantially reduces energy efficiency. Roller skating, as a low-impact locomotion modality, offers unique biomechanical advantages. Previous study has indicated that roller skating generates approximately 50% of the joint impact forces compared to running [5], with its smooth sliding motion significantly reducing workloads on the knee, hip and ankle joints. Thus, roller skating can leverage whole-body inertia to substantially minimize joint wear and energy dissipation while maintaining comparable traversing capabilities. This characteristic enables roller skating to be an efficient locomotion mode for extended operational endurance and joint longevity of humanoid robots. Therefore, this paper presents a newly developed humanoid robot, SKATER (Synthesized Kinematics for Advanced Traversing Efficiency

The authors are with the Institute of Humanoid Robots, Department of Precision Machinery and Precision Instrumentation, University of Science and Technology of China, Hefei, Anhui 230026, China. weigao@ustc.edu.cn; swzhang@ustc.edu.cn

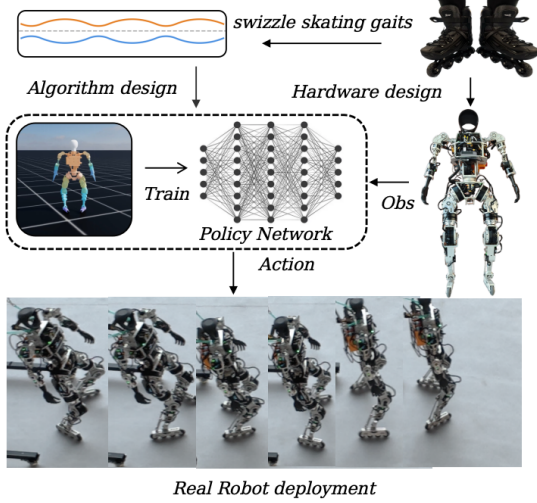


Fig. 1: The SKATER system: a humanoid robot equipped with roller skates for learning swizzle locomotion through deep reinforcement learning.

on a humanoid Robot), that is capable of roller skating with its special foot structure design, as shown in Fig. 1.

However, performing roller skating maneuver on humanoid platforms presents numerous control challenges. First, roller skating violates the fundamental assumption of static contact between stance foot and ground in traditional bipedal locomotion control [6]. Continuous foot sliding during the stance phase drastically compromises system stability and significantly complicates balance control. Second, roller skating involves intricate nonholonomic constraints, where wheels can only roll along specific directions without lateral sliding, introducing additional complexity to motion planning and control. Third, roller skating requires precise coordination of centroidal dynamics, leg swing and sliding motions. Existing research on roller skating has primarily focused on quadrupedal platforms, with limited studies on bipedal roller skating robots. Traditional model-based control approaches require precise modeling of friction forces, contact forces, and other physical parameters that are difficult to obtain accurately, and demonstrate poor adaptability to environmental disturbances. Furthermore, existing studies on bipedal roller skating robots predominantly rely on trajectory planning methods [7], [8], which suffer from low skating speeds and insufficient success rates. Additionally, roller skating on bipedal humanoid robots remains not fully explored.

To address the aforementioned challenges, this paper proposes a deep reinforcement learning (DRL) [9] based control framework for roller skating on SKATER. Specifically, tailored to the dynamic characteristics of roller skating, an implicit gait reward function is designed to guide the agent in learning the swizzle skating gaits. Additionally, a multi-stage curriculum learning strategy is employed to progressively increase task complexity during training. With the help of domain randomization techniques, the obtained control policy ultimately achieves successful sim-to-real transfer and deployment on SKATER.

The main contributions of this paper are:

- A newly developed 25-degree-of-freedom (DoF) humanoid robot, SKATER, with four passive inline wheels at each sole for roller skating.
- A deep reinforcement learning framework that integrates implicit gait reward function and multi-stage training curriculum for swizzle skating on SKATER.
- Comprehensive experimental study on SKATER performing maneuverable swizzle skating behaviors. Reduced Cost of Transport (CoT) and increased joint motion smoothness comparing to nominal bipedal walking gaits at equivalent forward velocities are observed.

II. RELATED WORK

A. Roller Skating Locomotion in Legged Robots

Previous study from Itabashi *et al.* [7] has developed a bipedal robot equipped with variable-curvature roller skating mechanisms, employing fifth-order Bézier curves for trajectory planning to achieve swizzle skating gaits. However, this method relies solely on position control, resulting in low system robustness and poor environmental adaptability. To address this limitation, Hashimoto *et al.* [8] propose a swizzle skating control method for a bipedal robot with passive wheels by analyzing the anisotropic friction characteristics between rolling and lateral directions to establish a mechanical model for swizzle skating. This approach introduces a reference trajectory modulation mechanism based on ground reaction forces at the foot, where the rate of foot reference position variation is dynamically adjusted accordingly, thereby effectively suppressing excessive internal forces induced by friction constraints and eventually achieving stable and continuous swizzle skating behaviors. Another study from Iverach-Brereton *et al.* designs the Jennifer robot [10] and adopts model-based control methods to overcome the dependence of Zero Moment Point (ZMP) on forward ground reaction forces, enabling roller skating on both ice and normal ground. However, experimental results indicate limitations in skating velocity and success rate.

In recent years, roller skating control research on quadrupedal platforms has flourished. The ETH research team has developed a motion planning and control framework for a modified version of the ANYmal quadrupedal robots that is capable of executing roller skating locomotion [11]. To address the nonholonomic constraint characteristics of roller skating, this framework replaces the

traditional friction cone model with a friction triangle model and employs hierarchical force control strategies for whole-body motion. Compared to conventional gaits, the Cost of Transport is reported to be reduced by over 80%. Chen *et al.* [12] also design a novel quadrupedal robot with 4-DoF legs that are equipped with passive wheels, capable of walking and various roller skating gaits. A geometrically characterized passive wheel model is proposed to improve contact point position accuracy in roller skating kinematics, and a controller based on the Levenberg-Marquardt method is developed for diverse roller skating gaits with small turning radii. Despite these significant advances, research on roller skating of humanoid robots remains relatively sparse in recent years, leaving substantial space for exploration.

B. Gait Generation and Learning-Based Control for Humanoid Robots

The Zero Moment Point (ZMP) criterion [13] and Model Predictive Control (MPC) method [14] have long constituted the predominant framework for humanoid locomotion control. These methods typically ensure dynamic stability by explicitly planning Center of Mass (CoM) trajectories and foothold locations while incorporating system dynamics and contact constraints. Although they offer excellent physical interpretability and engineering reliability, their performance is highly contingent on the accuracy of dynamic models and predefined assumptions regarding contact phase and state switching. Such dependencies often limit their applicability to high-dimensional systems or complex environments.

On the other hand, Deep Reinforcement Learning has gradually gain popularity for high-dimensional system control. Several previous studies have sought a combination of model and learning-based approaches. For instance, the MIT team utilize the Linear Inverted Pendulum (LIP) model to predict desired footholds and subsequently a trained DRL policy for precise foothold tracking [15]. While these hybrid methods leverage both physical priors and learned policies, they remain constrained by the explicit model assumptions regarding gait structure, phase segmentation and foothold reachability. Furthermore, some researchers have introduced auxiliary variables, such as step frequency or phase, to provide heuristic gait guidance [1]. Although the convergence challenges of pure end-to-end learning can be mitigated, the resulted gaits are still constrained by the predefined temporal or structural priors introduced.

Recent studies have suggested that for locomotion with distinct periodic characteristics, stable gaits do not necessarily require explicit phase modeling or reference trajectory tracking. By designing a reward function grounded in physical consistency, geometric constraints and kinematic symmetry, DRL can spontaneously yield stable periodic patterns. For example, Peng *et al.* have successfully generated natural walking gaits by introducing bilateral symmetry rewards without explicitly specifying gait timing [16], which offers a more flexible and general approach for complex humanoid systems. Additionally, the Humanoid-Gym framework in Isaac Gym [1] has emerged as a pivotal technical route

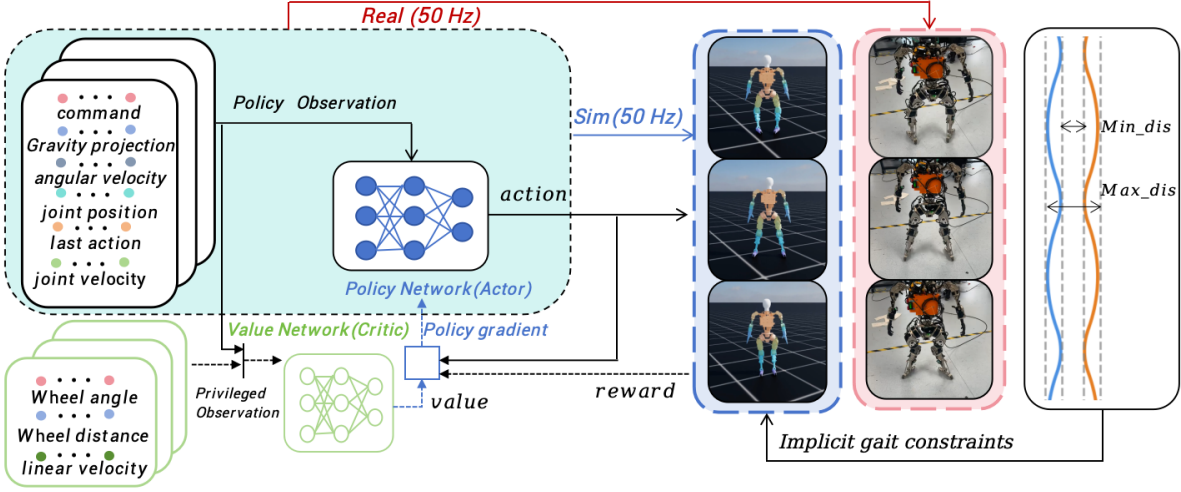


Fig. 2: Deep reinforcement learning control framework for SKATER. The policy network processes proprioceptive and exteroceptive sensor data to generate joint-level commands, enabling adaptive roller skate swizzle locomotion.

for large-scale parallel simulation, which enables learning stable locomotion policies within a short training duration and achieving successful zero-shot sim-to-real transfer.

For SKATER proposed in this paper, the non-holonomic constraints between the passive wheels and the ground further diminish the applicability of traditional phase-based or foot-trajectory-tracking methods. Therefore, an implicit gait guidance strategy based on inter-leg geometric relationships, motion symmetry and physical consistency constraints can demonstrate superior modeling flexibility and generalization potential.

III. METHODOLOGY

A. Hardware Design

As briefly mentioned in the Introduction, SKATER is a humanoid robot for roller skating locomotion, which has 33 degrees of freedom in total, as illustrated in Fig. 3. The 25 actuated degrees of freedom include 6 DoFs per leg, 5 DoFs per arm, 2 DoF in the waist and 1 DoF in the neck. Each foot is equipped with 4 roller skating wheels in linear configuration. The robot has a total mass of 38 kg and a standing height of 140 cm. An ASUS NUC mini-PC is equipped as the main computation resource and communicate with all 25 motors in real time through 5 EtherCAT-CAN conversion modules. Besides, an Xsens MTi-630R nine-axis Inertial Measurement Unit (IMU) is also connected to the NUC for state feedback. The operation commands are sent to the robot via an open-source ELRS remote controller.

The roller skating foot mechanism represents the core innovation of SKATER. Unlike traditional humanoid robots that employ either rigid flat feet or actuated wheels, SKATER uses a specifically optimized roller skating mechanism. Note that roller skate shoes are not directly utilized based on two critical considerations: 1) Roller skate shoes exhibit incompatibility to nominal rigid flat foot structures, because their outer shells introduce a compliant layer that is attached

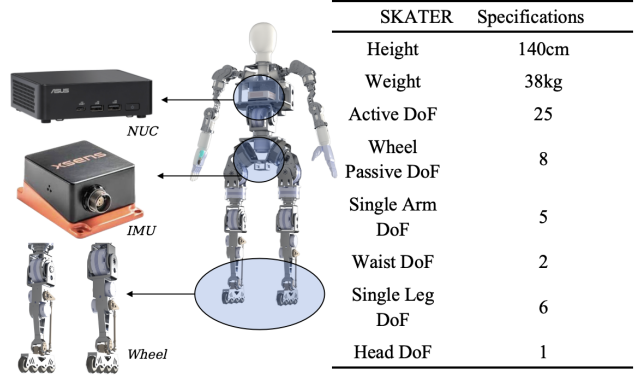


Fig. 3: Hardware specifications of the SKATER humanoid robot.

to the robot sole and can cause relative sliding, which compromises force transmission accuracy and position control precision. 2) The posterior structures of roller skate shoes interfere with the parallel-link transmission mechanism of the robot's ankle joints, limiting its range of motion during the highly flexible roller skating gaits. As a result, SKATER adopts polyurethane wheels with a diameter of 62 mm, whereas standard roller skate shoes commonly use wheels of diameters within 72-80 mm. The smaller wheel diameter can lower the foot CoM and reduce the moment load on the ankle roll axis. This optimization is particularly critical during the lateral propulsion phase of roller skating, where the ankle joint must withstand significant eversion and inversion moments.

B. Reinforcement Learning for Humanoid Locomotion

1) *Problem Formulation:* We formulate the roller skating problem of humanoid robots as a finite-horizon Markov Decision Process (MDP) [17], defined by the tuple $\mathcal{M} = \langle \mathcal{S}, \mathcal{A}, \mathcal{T}, \mathcal{R}, \gamma \rangle$. At each time step t , the robot observes a

state $s_t \in \mathcal{S}$ from the environment and executes an action $a_t \in \mathcal{A}$ generated by the policy $\pi_\theta(\cdot|s_t)$. Subsequently, the agent observes a successor state $s_{t+1} \sim \mathcal{T}(\cdot|s_t, a_t)$ according to the environment transition function \mathcal{T} , and receives a reward signal $r_t \in \mathcal{R}$.

The MDP is then solved using reinforcement learning methods [9], where the objective is to learn an optimal policy π_θ^* that maximizes the expected cumulative return over an episode of length T , *i.e.*,

$$\max_{\pi_\theta} \mathbb{E}_{\pi_\theta} \left[\sum_{t=0}^{T-1} \gamma^t r_t \right] \quad (1)$$

where $\gamma \in [0, 1]$ is the discount factor. The expected return is estimated by a value function (critic) V_ϕ . The training process is conducted in the IsaacLab simulator [18], employing the Proximal Policy Optimization (PPO) algorithm [19] with 4096 parallel simulation environments. To improve training stability, all input observations are normalized.

2) *Observation Space*: The Actor network takes as input the robot's current state along with states from 4 historical time steps, and outputs the desired joint PD control residual target values. The Actor's observation can be expressed as

$$o_t^{\text{actor}} = [s_t, s_{t-1}, s_{t-2}, s_{t-3}, s_{t-4}] \quad (2)$$

with the single-step state s_t is defined as

$$s_t = [q_t, \dot{q}_t, \omega_t, g, v_t^{\text{cmd}}, a_{t-1}] \quad (3)$$

where

- $q_t \in \mathbb{R}^{n_j}$: joint positions, where n_j denotes the number of controllable joint degrees of freedom
- $\dot{q}_t \in \mathbb{R}^{n_j}$: joint velocities
- $\omega_t \in \mathbb{R}^3$: robot body angular velocity
- $g \in \mathbb{R}^3$: gravity vector projected in the robot base coordinate frame
- $v_t^{\text{cmd}} \in \mathbb{R}^3$: user command velocity (including linear and angular velocities)
- $a_{t-1} \in \mathbb{R}^{n_j}$: action output from the previous time step

Note that the wheel joints are excluded from the observations because they are passively rotated to accommodate ground motion and their states are naturally determined by system dynamics. By incorporating a historical observation window, the Actor can implicitly model the dynamic characteristics and inertial effects of motion, thereby generating smoother and more stable control actions.

During training, the Critic has access to additional privileged information as

$$o_t^{\text{critic}} = [v_t^{\text{lin}}, d_t^{\text{ankle}}, \theta_t^{\text{ankle}}] \quad (4)$$

where

- $v_t^{\text{lin}} \in \mathbb{R}^3$: actual base linear velocity (ground truth)
- $d_t^{\text{ankle}} \in \mathbb{R}$: distance between the two ankle joints
- $\theta_t^{\text{ankle}} \in \mathbb{R}^2$: orientation angles of the left and right ankle joints with respect to the base's x -axis (forward direction)

3) *Action Space*: A torque-based PD controller is employed for joint actuation. The action a_t represents the difference between the current and the next-step joint position. The desired position is then expressed as

$$p_t^d = p_t + \beta a_t \quad (5)$$

where each dimension of a_t is constrained within the range $[-1, 1]$. The action scaling coefficient β bounds the action limits, thereby implicitly regulating the motion velocity. The joint torque at time step t is computed as

$$\tau_t = K_p \cdot (p_t^d - p_t) - K_d \cdot \dot{p}_t \quad (6)$$

where K_p and K_d denote the proportional and derivative gains of the PD controller, respectively.

4) *Reward Function*: The reward function for roller skating differs fundamentally from traditional bipedal walking. While the latter primarily relies on gait cycles and foot contact patterns, the former requires maintaining continuous wheel-ground sliding motion. Consequently, a multi-objective reward function comprising 22 reward terms is specifically designed for roller skate swizzle to balance task completion and motion constraints. Note that our reward function design does not explicitly introduce kinematic trajectories or gait timing constraints for swizzle. Instead, only necessary physical constraints and motion preferences are provided through boundary constraints on inter-foot distance (minimum 0.2 m and maximum 0.5 m) and limb symmetry rewards. This setup sees natural emergence of swizzle gaits during the training process, and enhanced adaptability and robustness during physical deployment, eliminating the need for meticulous manual reward design tailored to specific gaits. The detailed specifications of each reward term are provided in Table I.

C. Sim-to-Real Gap

The sim-to-real transfer gap constitutes one of the key challenges in reinforcement learning for physical robots. This work tackles this gap from two perspectives. The dynamic parameters of the physical robot, such as damping coefficients and moments of inertia, are first carefully calibrated using system identification methods. Then during the training process, domain randomization techniques are further employed to mitigate the impact of the uncalibrated physical parameter discrepancies. Details about the domain randomization parameters can be found in Table II.

IV. EXPERIMENTS

To evaluate the performance of roller skate swizzle, nominal bipedal walking gaits are also tested on SKATER with the passive wheel mechanism replaced by normal rigid flat foot. The walking algorithm used the open-source `unitree_rl.lab` framework [20] from Unitree Robotics. The learned policy is first deployed in the MuJoCo physics engine for sim-to-sim tests given its high-precision foot contact force simulation, and then deployed on SKATER for sim-to-real evaluation.

TABLE I: Reward Function

Reward Term	Formula	Weight
Task Rewards		
Linear Velocity Track	$\exp\left(-\frac{\ \mathbf{v}_{xy}^{\text{cmd}} - \mathbf{v}_{xy}^{\text{base}}\ ^2}{\sigma^2}\right)$	3.2
Angular Velocity Track	$\exp\left(-\frac{(\omega_z^{\text{cmd}} - \omega_z^{\text{base}})^2}{\sigma^2}\right)$	1.2
Alive	Constant	0.15
Base Penalties		
Angular Velocity XY	$-\ \boldsymbol{\omega}_{xy}^{\text{base}}\ ^2$	-0.05
Joint Velocity	$-\ \dot{\mathbf{q}}\ ^2$	-0.001
Joint Acceleration	$-\ \ddot{\mathbf{q}}\ ^2$	-2.5×10^{-7}
Action Rate	$-\ \mathbf{a}_t - \mathbf{a}_{t-1}\ ^2$	-0.05
Joint Position Limits	$-\sum_i \max(0, q_i - q_i^0 - \ell_i)^2$	-5.0
Energy	$-\sum_i \tau_i \dot{q}_i $	-2×10^{-5}
Joint Penalties		
Arms Deviation	$-\sum_{\text{arms}} q_i - q_i^0 $	-0.4
Waist Deviation	$-\sum_{\text{waist}} q_i - q_i^0 $	-2.0
Head Deviation	$-\ q_{\text{head}} - q_{\text{head}}^0\ $	-1.0
Ankle Roll Deviation	$-\sum_{\text{ankle}} q_i - q_i^0 $	-0.2
Posture Penalties		
Flat Orientation	$-\ \mathbf{g}_{\text{proj}} - [0, 0, -1]^T\ ^2$	-7.0
Base Height	$-(h_{\text{base}} - h_{\text{target}})^2$	-2.0
Foot Constraints		
Feet Too Near	$-\mathbb{I}(d_{\text{feet}} < 0.2m)$	-1.0
Feet Too Far	$-\mathbb{I}(d_{\text{feet}} > 0.5m)$	-5.0
Wheel Penalties		
Wheel Axial Slip	$-\sum_{\text{wheels}} v_{\text{axial}} $	-0.1
Wheel Air Time	$-\mathbb{I}(n_{\text{contact}} < n_{\text{min}})$	-1.0
Symmetry Rewards		
Leg Symmetry	$-(w_q \ \mathbf{q}_L - \mathbf{q}_R\ ^2 + w_v \ \dot{\mathbf{q}}_L - \dot{\mathbf{q}}_R\ ^2)$	0.5
Arm Symmetry	$-(w_q \ \mathbf{q}_L - \mathbf{q}_R\ ^2 + w_v \ \dot{\mathbf{q}}_L - \dot{\mathbf{q}}_R\ ^2)$	0.5
Contact Penalties		
Undesired Contacts	$-\sum_{\text{body}} \mathbb{I}(F_{\text{contact}} > 1.0N)$	-1.0

A. Simulation Results

1) *Contact Force Analysis*: Fig. 4 presents a temporal comparison of vertical Ground Reaction Forces (GRF) between the swizzle gait and the walking gait at the commanded speed of 1 m/s. Given the weight of SKATER being approximately 372.4 N, it can be seen that nominal walking generates pronounced impact peaks at each heel strike, with peak forces reaching 1.5-2.0 times body weight and impact durations being as brief as approximately 50-100 ms, imposing substantial loads on the joints. In contrast, the force profile of the swizzle gait exhibits smooth periodic variations. Excluding the startup phase where the robot must exert force to acquire acceleration, the peak forces are reduced to 1.1-1.3 times body weight with significantly decreased force variation rates.

To further quantify the impact severity, we define an Impact Intensity metric as:

$$I = \frac{1}{T} \int_{t_0}^{t_f} \left| \frac{dF_z}{dt} \right| dt \quad (7)$$

Consequently, the impact intensity for the walking gait is $I_{\text{bipedal}} = 10231.42$ N/s, while that for the swizzle gait is

TABLE II: Domain Randomization Parameters

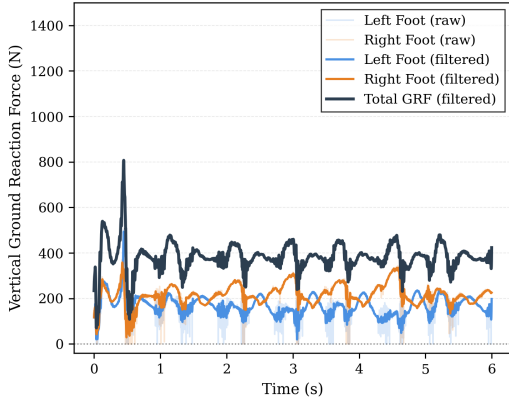
Term	Value
Physics Material - Wheels	
Static Friction	$\mathcal{U}(0.1, 0.8)$
Dynamic Friction	$\mathcal{U}(0.1, 0.4)$
Restitution	0.0
Link Mass	$\mathcal{U}(0.9, 1.1) \times \text{default kg}$
Center of Mass Offset	
x-axis	$\mathcal{U}(-0.01, 0.01)$ m
y-axis	$\mathcal{U}(-0.01, 0.01)$ m
z-axis	$\mathcal{U}(-0.01, 0.01)$ m
Actuator Gains	
Stiffness	$\mathcal{U}(0.9, 1.1) \times \text{default}$
Damping	$\mathcal{U}(0.9, 1.1) \times \text{default}$
Joint Damping - Wheels	$\mathcal{U}(0.002, 0.005)$ N·m·s/rad

$I_{\text{roller}} = 2469.44$ N/s, which is a reduction of approximately 75.86% and indicates the significant advantage of roller skating locomotion in reducing joint impact loads.

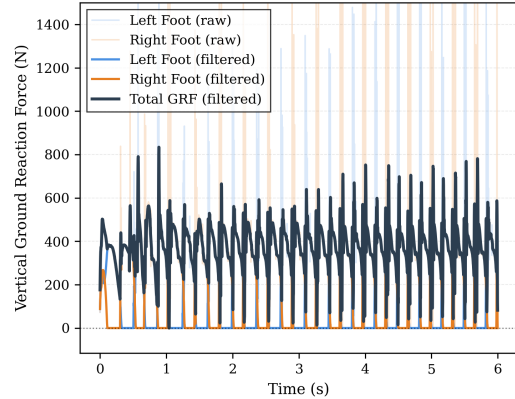
2) *Velocity Tracking Performance*: To evaluate SKATER's velocity tracking performance, experiments with variable forward velocity are carried out in MuJoCo. The desired velocity sequence was set to 0.6, 1.2, 1.8, 1.2, 0.6, 0.0 m/s, with switching intervals being 2.0 s. Fig. 5 presents the velocity tracking performance of the robot.

During acceleration phases, the robot must increase leg propulsion force to acquire forward acceleration, resulting in certain spikes at velocity transitions. Overall, the results indicate that the robot possesses reasonable velocity tracking capability, but exhibits two significant issues: one is the actual velocity consistently exceeds the desired velocity, manifesting steady-state tracking errors, and the other is the response during deceleration phases is sluggish. These phenomena indicate the inherent limitations of roller skating in velocity control compared to bipedal walking. While bipedal walking can achieve precise velocity tracking by modulating ground reaction forces via stance foot and discrete footholds via swing foot, roller skating relies on continuous sliding motion to track forward velocity. As a result, the robot cannot rapidly adjust velocity in roller skating through foot braking as in normal walking, and requires longer response time for velocity adjustment. Additionally, velocity control in roller skating is highly dependent on the ground friction coefficient. Therefore, specialized velocity tracking control strategies tailored to the physical characteristics of roller skating are desired in the future work.

3) *Gait Pattern Visualization*: For a swizzle gait, Fig. 6a displays the trajectories of left and right foot in the horizontal plane, exhibiting the characteristic "swizzle-shaped" periodic path, Fig. 6b shows the bounded distance variation between the feet, and Fig. 6c presents the temporal evolution of both ankle angles, demonstrating favorable periodic coordination. These results demonstrate that through appropriately designed constraints and reward terms, DRL can autonomously discover and optimize swizzle gaits without relying on manually designed reference trajectories or state machines. This



(a)



(b)

Fig. 4: Comparison of foot contact force profiles: (a) roller skating locomotion with continuous ground contact and stable force distribution, and (b) conventional bipedal walking with periodic impact peaks and zero-force swing phases.

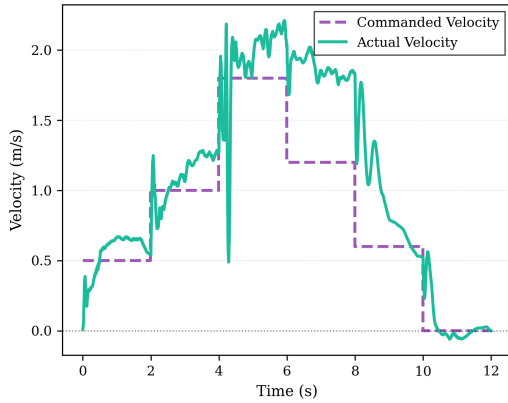


Fig. 5: Velocity tracking performance of SKATER following step reference commands.

data-driven approach provides a novel way for roller skating locomotion control of bipedal humanoid robots.

B. Hardware Results

The learned control policy is then transferred to the physical robot for real world evaluation. The policy inference runs at 50 Hz on the onboard mini-PC to demonstrate its efficacy.

1) *Locomotion Performance Testing*: To validate the basic locomotion capabilities of the robot, three experiments were designed in this work: forward sliding (Fig. 7a), backward sliding (Fig. 7b) and forward obstacle-crossing sliding (Fig. 7c). In each experimental trial, the robot initiated from a stationary state, then accelerated and finally braked stably through pigeon-toed stance. The forward and backward sliding experiments can demonstrate the stability and control precision of linear motion, while the forward obstacle-crossing experiment can validate the robot’s traversability in unstructured environments. Experimental results demonstrate that the proposed control strategy can effectively realize omnidirectional locomotion control, with the robot exhibit-

TABLE III: Performance Evaluation on Different Surface Types

Surface Type	Friction Coefficient	Trials (Success)
Tile Floor	0.2–0.4	10/10 (100%)
Rubber Floor	0.5–0.7	10/10 (100%)
Gravel Pavement	0.8–1.0	10/10 (100%)

ing satisfying stability and maneuverability across various motion modes.

2) *Multi-Friction Terrain Testing*: To evaluate the robot’s adaptability to different ground surfaces, tests were conducted on three typical ground types with various friction coefficients, including tile (Fig. 8a), rubber (Fig. 8b) and gravel pavement (Fig. 8c). On each surface type, the robot performed 10-meter straight-line roller skate swizzle for 10 repeated trials. The results are summarized in Table III.

The experimental results indicate that SKATER achieved a 100% success rate across all tested surfaces, demonstrating excellent terrain adaptability. Despite significant differences in friction coefficients among the three surface types, the trained control policy can adaptively adjust skating motions to maintain stable locomotion performance, validating the strong robustness of the proposed method.

3) *Joint Impact Load Evaluation*: To quantitatively assess the mechanical impact of walking and swizzle gaits on robot joints, joint torque data were collected from SKATER with both locomotion gaits at a commanded speed of 1 m/s. Peak torque is employed as the evaluation metric, with focus mainly on the dynamic characteristics of the 12 lower-limb joints. Table IV presents the detailed results.

Table IV indicate that the roller skate swizzle gait significantly reduces peak torques across most joints. Notably, the torque reductions are most pronounced in the hip pitch and ankle pitch joints, reaching 74% and 65% – 75%, respectively. This is attributed to the continuous sliding motion in the swizzle gait, which avoids the periodic impact at touchdown from the walking gait. These results validate that the roller skating mode can effectively extend robot

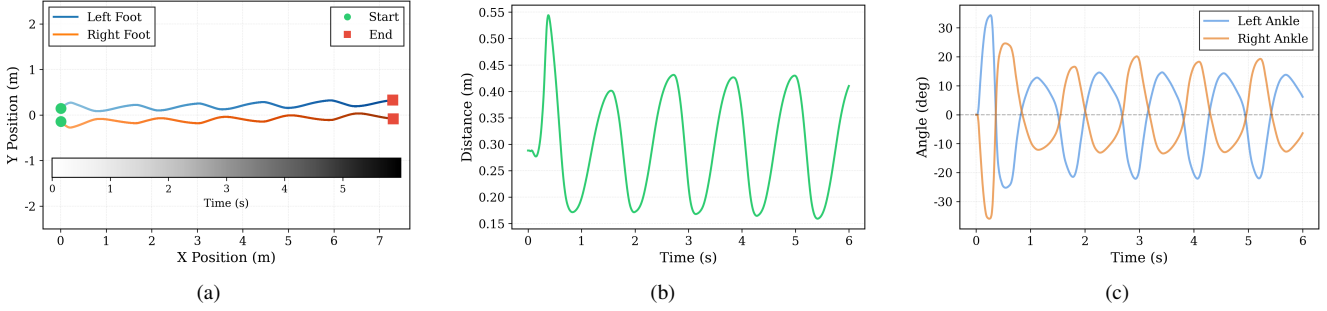


Fig. 6: Analysis of foot-end kinematics during locomotion: (a) 2D trajectory map in the workspace; (b) variation of inter-foot distance over time; (c) dynamic profiles of the ankle joint angle.

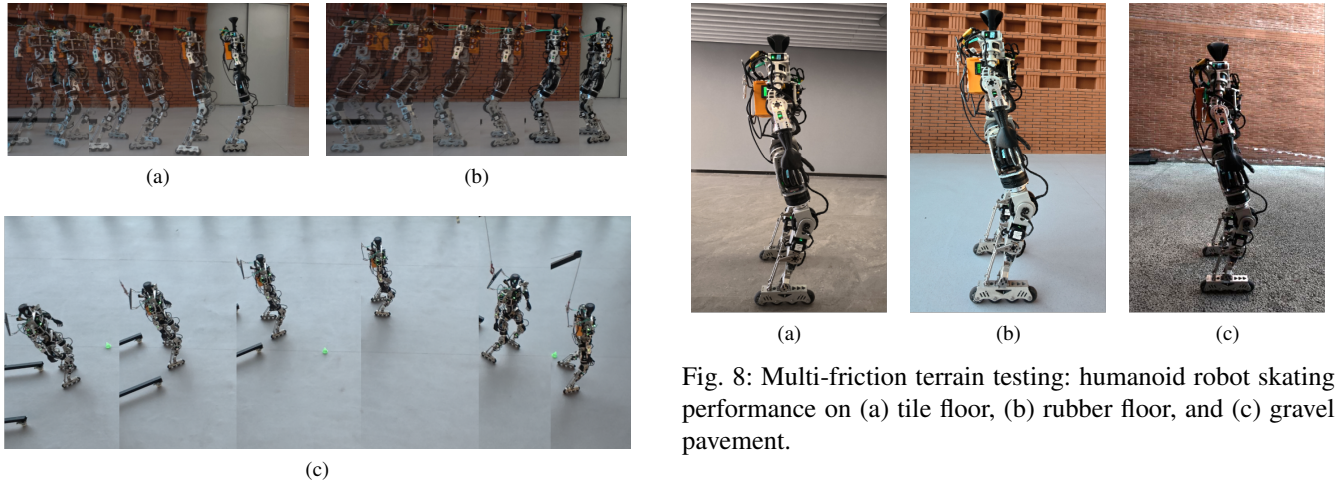


Fig. 7: Experimental validation of robot mobility: (a) forward sliding, (b) backward sliding, and (c) turning maneuver.

TABLE IV: Comparison of Peak Joint Torques Between Skating and Walking Modes

Joint Name	Skating(N·m)	Walking(N·m)	Difference (%)
L Hip Pitch	17.91	70.38	-74.56
L Hip Roll	58.69	60.22	-2.54
L Hip Yaw	22.94	32.98	-30.45
L Knee	45.51	44.87	+1.43
L Ankle Pitch	12.23	48.62	-74.85
L Ankle Roll	9.56	9.64	-0.83
R Hip Pitch	17.14	66.03	-74.04
R Hip Roll	58.21	74.60	-21.97
R Hip Yaw	24.14	37.80	-36.14
R Knee	43.91	45.84	-4.21
R Ankle Pitch	14.48	40.78	-64.50
R Ankle Roll	11.45	11.32	+1.15

service life and reduce maintenance costs by diminishing joint impact loads, demonstrating the superiority of this locomotion approach.

4) Cost of Transport Comparison: Note that although in the bipedal walking gaits, the foot mechanisms with passive wheels of SKATER are replaced by rigid flat feet, the sensor and actuator configurations of the robot remain consistent in both locomotion modes, thus the total mass variation of the

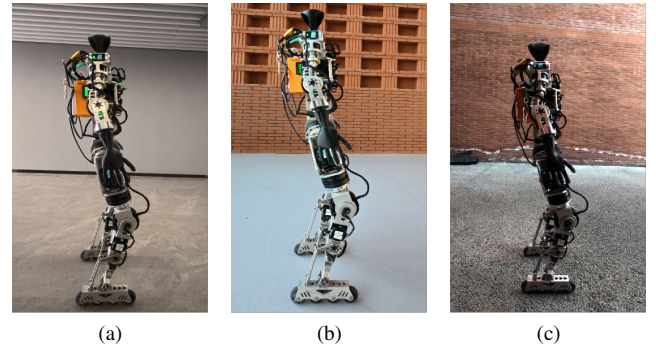


Fig. 8: Multi-friction terrain testing: humanoid robot skating performance on (a) tile floor, (b) rubber floor, and (c) gravel pavement.

robot is less than 1%, resulting in a fair comparison of energy efficiency. For each locomotion mode, the robot travels 15 meters in a straight line at a commanded speed of 1 m/s for 5 repeated trials to ensure statistical significance. Given that the host computer power consumption and sensor power consumption remain constant across both modes, this work focuses on the pure energy consumption for locomotion, with the CoT calculated as [21]

$$\text{CoT} = \frac{\sum_{i=1}^n \left(\int_{t_0}^{t_f} |\tau_i \cdot \omega_i| dt \right)}{M \cdot g \cdot D} \quad (8)$$

where τ_i is the torque of the i -th joint, ω_i is the corresponding angular velocity, M is the robot mass, g is gravitational acceleration, D is the travel distance, and n is the total number of joints.

Fig. 9 presents the CoT comparison results under both locomotion modes, which illustrates that the swizzle gait achieves a 63.34% reduction in CoT compared to the walking gait. Specifically, the Hip Pitch joint that consumes the most energy during walking experiences an energy consumption reduction by approximately 95.39% during swizzling. Similarly, the Ankle Pitch joint also exhibits a 92.29% reduction in energy consumption. The remaining joints see relatively smaller variations. Overall, the swizzle gaits have achieved significant energy efficiency improvements compared to tra-

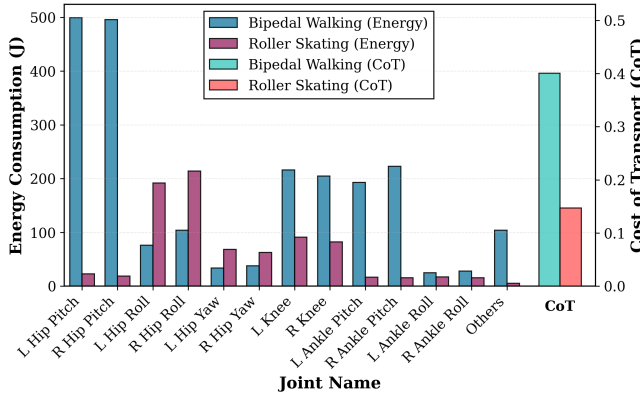


Fig. 9: Energy efficiency analysis of humanoid robot locomotion: Cost of transport comparison and joint-level energy consumption between skating and walking modes.

ditional bipedal walking gaits. The swizzle gaits can effectively exploit passive dynamics and momentum conservation principles, transforming the robot's locomotion pattern from discrete stance-swing phases to continuous sliding motion, reducing energy consumption by diminishing the actuation demands of sagittal plane joints. It demonstrates that our roller skating humanoid robot can possess higher energy utilization efficiency in long-distance locomotion tasks, leading to enhanced endurance in practical application scenarios.

V. CONCLUSION

This paper proposes a 25-DoF humanoid robot, SKATER, equipped with roller skate mechanism at both feet, and a corresponding deep reinforcement learning control framework for roller skating locomotion. Through multi-stage training curriculum with carefully designed reward function design and adequate domain randomization techniques, SKATER has successfully achieved efficient and smooth swizzle gaits in both simulation and physical experiments, exhibiting significant advantages over traditional bipedal walking gaits. Simulation analysis has revealed a 75.86% reduction in contact force impact intensity, while real robot experiments has shown a 63.34% reduction in Cost of Transport (CoT), with peak torques in hip and ankle joints reduced by approximately 74% and 70%, respectively. Additionally, the robot has achieved a 100% success rate with tests across ground surfaces with various friction coefficients, demonstrating strong control robustness of the learned policy.

Limitations of this study include lateral drift during straight-line skating, lag in velocity tracking response, and the realization of only swizzle gaits with continuous ground contact of both legs. Future work can proceed in three directions: 1) investigating high-dynamic gaits such as push steps and single-leg support to enhance maneuverability, 2) integrating perception to enable autonomous navigation in complex environments, and 3) exploring actively switchable passive wheel-foot mechanisms to further improve traversability.

REFERENCES

- [1] X. Gu, Y.-J. Wang, and J. Chen, "Humanoid-gym: Reinforcement learning for humanoid robot with zero-shot sim2real transfer," *arXiv preprint arXiv:2404.05695*, 2024.
- [2] Z. Li, X. B. Peng, P. Abbeel, S. Levine, G. Berseth, and K. Sreenath, "Reinforcement learning for versatile, dynamic, and robust bipedal locomotion control," *The International Journal of Robotics Research*, vol. 44, no. 5, pp. 840–888, 2025.
- [3] T. He, J. Gao, W. Xiao, Y. Zhang, Z. Wang, J. Wang, Z. Luo, G. He, N. Sobanbab, C. Pan *et al.*, "Asap: Aligning simulation and real-world physics for learning agile humanoid whole-body skills," *arXiv preprint arXiv:2502.01143*, 2025.
- [4] Z. Zhang, J. Guo, C. Chen, J. Wang, C. Lin, Y. Lian, H. Xue, Z. Wang, M. Liu, J. Lyu *et al.*, "Track any motions under any disturbances," *arXiv preprint arXiv:2509.13833*, 2025.
- [5] A. T. Mahar, T. R. Derrick, J. Hamill, and G. E. Caldwell, "Impact shock and attenuation during in-line skating," *Medicine and Science in Sports and Exercise*, vol. 29, no. 8, pp. 1069–1075, 1997.
- [6] R. Grandia, F. Jenelten, S. Yang, F. Farshidian, and M. Hutter, "Perceptive locomotion through nonlinear model-predictive control," *IEEE Transactions on Robotics*, vol. 39, no. 5, pp. 3402–3421, 2023.
- [7] K. Itabashi and M. Kumagai, "Development of a human type legged robot with roller skates," in *2010 IEEE/SICE International Symposium on System Integration*, 2010, pp. 120–125.
- [8] K. Hashimoto, Y. Sugahara, H. O. Lim, and A. Takanishi, "Swizzle movement for biped walking robot having passive wheels," *Journal of Robotics and Mechatronics*, vol. 20, no. 3, pp. 413–419, 2008.
- [9] C. Tang, B. Abbatecamteo, J. Hu, R. Chandra, R. Martín-Martín, and P. Stone, "Deep reinforcement learning for robotics: A survey of real-world successes," *Annual Review of Control, Robotics, and Autonomous Systems*, vol. 8, no. 1, pp. 153–188, 2025.
- [10] C. Iverach-Brereton, J. Baltes, J. Anderson, A. Winton, and D. Carrier, "Gait design for an ice skating humanoid robot," *Robotics and Autonomous Systems*, vol. 62, no. 3, pp. 306–318, 2014.
- [11] M. Bjelonic, C. D. Bellicoso, M. E. Tiriyaki, and M. Hutter, "Skating with a force controlled quadrupedal robot," in *2018 IEEE/RSJ International Conference on Intelligent Robots and Systems (IROS)*. IEEE, 2018, pp. 7555–7561.
- [12] J. Chen, R. Qin, L. Huang, Z. He, K. Xu, and X. Ding, "Unlocking versatile locomotion: A novel quadrupedal robot with 4-dofs legs for roller skating," in *2024 IEEE International Conference on Robotics and Automation (ICRA)*. IEEE, 2024, pp. 8037–8043.
- [13] M. Vukobratović and B. Borovac, "Zero-moment point—thirty five years of its life," *International journal of humanoid robotics*, vol. 1, no. 01, pp. 157–173, 2004.
- [14] S. Katayama, M. Murooka, and Y. Tazaki, "Model predictive control of legged and humanoid robots: models and algorithms," *Advanced Robotics*, vol. 37, no. 5, pp. 298–315, 2023.
- [15] H. J. Lee, S. Hong, and S. Kim, "Integrating model-based footstep planning with model-free reinforcement learning for dynamic legged locomotion," in *2024 IEEE/RSJ International Conference on Intelligent Robots and Systems (IROS)*. IEEE, 2024, pp. 11 248–11 255.
- [16] X. B. Peng, G. Berseth, K. Yin, and M. Van De Panne, "Deeploco: Dynamic locomotion skills using hierarchical deep reinforcement learning," *Acm transactions on graphics (tog)*, vol. 36, no. 4, pp. 1–13, 2017.
- [17] M. L. Puterman, *Markov decision processes: discrete stochastic dynamic programming*. John Wiley & Sons, 2014.
- [18] M. Mittal, P. Roth, J. Tigue, A. Richard, O. Zhang, P. Du, A. Serrano-Muñoz, X. Yao, R. Zurbrügg, N. Rudin *et al.*, "Isaac lab: A gpu-accelerated simulation framework for multi-modal robot learning," *arXiv preprint arXiv:2511.04831*, 2025.
- [19] J. Schulman, F. Wolski, P. Dhariwal, A. Radford, and O. Klimov, "Proximal policy optimization algorithms," *arXiv preprint arXiv:1707.06347*, 2017.
- [20] Unitree Robotics, "unitree_rl_lab: A repository for reinforcement learning implementation for unitree robots, based on isaclab," https://github.com/unitreerobotics/unitree_rl_lab, 2024, accessed: 2025-12-25.
- [21] Y. G. Alqaham, J. Cheng, and Z. Gan, "Energy-optimal asymmetrical gait selection for quadrupedal robots," *IEEE Robotics and Automation Letters*, 2024.